

Synthesis and characterizations of CdS nanorods by SILAR method: effect of film thickness

D. S. Dhawale · D. P. Dubal · M. R. Phadatare ·
J. S. Patil · C. D. Lokhande

Received: 3 November 2010 / Accepted: 26 February 2011 / Published online: 15 March 2011
© Springer Science+Business Media, LLC 2011

Abstract In this investigation, we have successfully synthesized CdS nanorods by simple and inexpensive successive ionic layer adsorption and reaction (SILAR) method. The effect of film thickness on the physico-chemical properties such as structural, morphological, wettability, optical, and electrical properties of CdS nanorods has been investigated. The XRD pattern revealed that CdS films are polycrystalline with hexagonal crystal structure. SEM and TEM images showed that CdS film surface are composed of spherical grains along with some spongy cluster and an increase in film thickness up to 1.23 μm causes the formation of matured nanorods having diameter 150–200 nm. The increases in water contact angle form 105° to 130° have been observed as film thickness increases from 0.13 to 1.23 μm indicating hydrophobic nature. The optical band gap was found to be increased from 2.02 to 2.2 eV with increase in film thickness. The films showed the semiconducting behavior with room temperature electrical resistivity in the range of 10⁴–10⁶ Ω cm and have n-type electrical conductivity.

Introduction

In recent years, significant research effort has been devoted to developing inorganic nanocrystals because of their potential application in biology, electronics, optics, transport, and information technology. Although, several

approaches investigated ways of making these nanocrystalline thin films, controlling the size, shape, and crystallinity and various parameters affecting the size and shape of these materials still need to be found [1]. As an important II–IV compound semiconductor material with wide band gap energy of 2.4 eV (in bulk), CdS has attracted much attention because of their novel properties and possible application in both optoelectronic and biological fields [2–6]. CdS nanoparticles are attractive candidate for optoelectronic application as it is possible to tailor the band gap over wide spectral range (visible to UV). CdS is a technologically useful material, as many devices based on CdS, including sensors have come up in the recent years. The thin film CdS solar cell has for several years been considered to be a promising alternative to the more widely used silicon devices. The CdS thin film has an n-type electrical conductivity and is often used in optoelectronic devices, especially, in case of chalcopyrite heterojunction solar cells, it acts as buffer layer. In the conventional absorber-window configuration thin film heterojunction solar cells, n-CdS window have paired with p-Cu₂S, p-CdTe, and p-CuInSe₂ absorber layers to result in efficient solar cells. CdS has been employed in high efficiency solar cells formed with Cu₂S [7], Cu (In, Ga) Se₂ [8], and CdTe [9].

CdS in a nanocrystalline thin films form can be prepared by a variety of methods (both physical and chemical) like gas evaporation [10], micelles [11], electrodeposition [12], chemical bath deposition [13, 14], spray pyrolysis [15], and screen printing [16]. Recently, deposition of CdS thin films was carried out by a new chemical method having successive ionic layer adsorption and reaction (SILAR) [17–19]. In this method the substrate is immersed successively in separately placed cationic and anionic precursors and rinsing between each immersion with water. The SILAR method for preparation of thin films is simple,

D. S. Dhawale · D. P. Dubal (✉) · M. R. Phadatare ·

J. S. Patil · C. D. Lokhande

Thin Film Physics Laboratory, Department of Physics,
Shivaji University, Kolhapur 416 004, India
e-mail: dubal_deepak@yahoo.co.in

C. D. Lokhande

e-mail: l_chandrakant@yahoo.com

attractive, inexpensive, and less time consuming compared to other methods. Its main advantage is easy control over the growth rate through its various parameters viz., time, number of immersions, solution concentration, pH, etc.

In this study, CdS films of different film thickness were prepared by a standard SILAR method. The structural, morphological, wettability, optical, and electrical properties were investigated using XRD, SEM, TEM contact angle measurement, UV–Vis spectroscopy, and two-probe electrical resistivity. We also investigated the influence of the film thickness on properties of CdS thin films.

Experimental

CdS thin films have been deposited onto a glass substrate by alternate immersion of the substrate in cadmium acetate and sodium sulfide solutions, kept at room temperature (300 K). The pH of cadmium acetate and sodium sulfide solutions was ~ 5 and ~ 12 , respectively. The cleaned glass substrate was immersed in the 0.0125 M cadmium acetate solution for 20 s to get cadmium ions adsorbed on the substrate. To remove loosely bound Cd^{2+} ions, the substrate was rinsed in double distilled water for 10 s. Then the substrate was immersed in 0.05 M sodium sulfide solution for 20 s, where S^{2-} ions react with preadsorbed Cd^{2+} ions to form CdS thin film on the substrate. Again the substrate was immersed in double distilled water for 10 s to remove unreacted S^{2-} ions and loosely bound CdS material from the surface of glass substrate. Thus, one deposition cycle consists of 20 s adsorption of Cd^{2+} ions, 10 s rinsing in double distilled water, 20 s reaction of S^{2-} ions with preadsorbed Cd^{2+} ions on the substrate and again 10 s rinsing in double distilled water. Repeating such number of 140, 150, and 160 cycles, CdS thin films of different thickness were deposited on glass substrate.

The thickness of the CdS films was measured by a weight difference method using a sensitive microbalance. The crystal structure of the CdS thin films was identified by X-ray diffraction analysis with Philips (PW 3710) diffractometer using CrK_α radiation ($\lambda = 2.2897 \text{ \AA}$) in 2θ range from 20° to 100° . The surface morphology and particle size of the CdS films with corresponding selected area electron diffraction (SAED) were examined by FESEM (XL30 ESEM FEG) and transmission electron microscopy (TEM) (Philips CM-30 TEM unit, Point resolution = 2.4 \AA) with acceleration voltage of 300 kV coupled with EDAX-DX-4 analyzer, respectively. In the process of preparation of the TEM specimen, a small amount of the powders was dispersed in a few milliliters of normal butanol in an ultrasonic bath and sonicated for 30 min, and a drop from an eye dropper of this dispersion sample was placed on a copper grid coated with holey

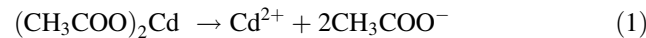
carbon film. The samples were placed in a vacuum oven to dry at ambient temperature before examining. Contact angle measurement was carried out by Rame-hart USA equipment with CCD camera. The optical absorption study was carried out over the wavelength range 450–850 nm using UV–Vis Systronics spectrophotometer-119, with glass substrate as a reference. The electrical resistivity of CdS film was measured using dc two-probe method in the temperature range 300–500 K. The brass block was used as a sample holder and chromel–alumel thermocouple was used to measure the temperature difference. The area of the film (1 cm^2) was defined and silver paste was applied in order to make good ohmic contact to CdS thin film. The type of electrical conductivity was determined from thermo-emf measurements.

Results and discussion

Film formation and reaction mechanism

CdS thin films were deposited by immersing glass substrates in separately placed cationic and anionic precursors with rinsing between every immersion. The growth mechanism of thin film deposition process is ion-by-ion at nucleation sites on the immersed surfaces. The mechanism of CdS film formation by SILAR method is explained as follows

The cationic precursor solution releases Cd^{2+} ions from cadmium acetate as,



In the anionic precursor solution, sodium sulfide releases S^{2-} ions as,



When the substrate is immersed in Cd^{2+} containing solution, Cd^{2+} ions are adsorbed on the surface of a glass substrate. After immersion of such substrate in S^{2-} ion containing solution, following reaction takes place on the surface of glass substrate,



Such cycles are repeated to form CdS thin film.

Thickness measurement

Film thickness is important parameter in the study of film properties. The thickness of the CdS films was measured by a gravimetric weight difference method, assuming the bulk density ($\rho = 8.15 \text{ g/cm}^3$) of the CdS. Figure 1 shows the film thickness variation with number of deposition cycles. The rate of increase of film thickness is nonlinear which

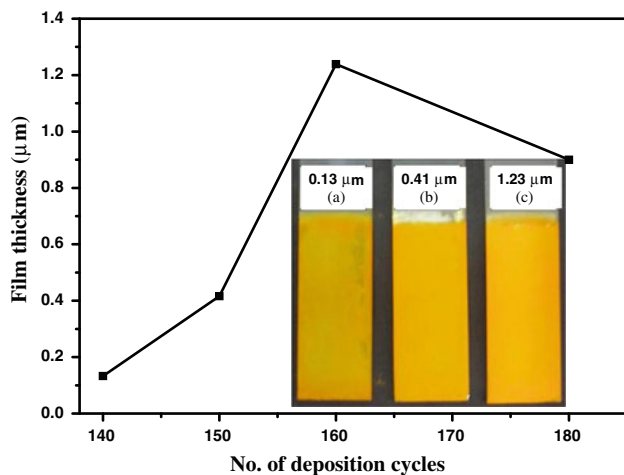


Fig. 1 The variation of CdS film thickness with the number of deposition cycles. Inset The photograph of CdS thin films of different thicknesses: (a) 0.13, (b) 0.41, and (c) 1.23 μm

indicates growth is due to nucleation and coalescence process. More nucleation sites contribute to coagulation during the growing procedure. Thicknesses of CdS films are found to be 0.13, 0.41, and 1.23 μm for 140, 150, and 160 cycles, respectively. With increasing the deposition cycles, increase in film thickness was observed. This may be due to sufficient reaction time period available for the formation of oriented growth of CdS thin films. Furthermore, after 160 cycles slight decrease in film thickness observed could be attributed to the formation of outer porous layer and/or the film which may develop stress to cause delamination, resulting in peeling off the film after the film reaches at maximum thickness [20]. Thus, the terminal thickness of CdS thin film was found to be 1.23 μm for 160 cycles. Inset of Fig. 1 shows photographs of CdS thin film at different thicknesses over $\sim 20 \text{ cm}^2$ area confirming the feasibility of SILAR method for large area deposition. The prepared CdS films were found to be well adherent, uniform and yellowish in color.

Structural studies

Figure 2a–c shows the XRD patterns of CdS thin films deposited for thicknesses as 0.13, 0.41, and 1.23 μm , respectively. The broad hump in XRD pattern is due to amorphous nature of glass substrate and as the film thickness increase, relative peak intensity also increases. It is evident from XRD pattern that CdS thin films are polycrystalline and has hexagonal crystal structure similar to the results reported elsewhere [18, 21]. The XRD pattern indicates the presence of (100), (002), (101), and (110) planes of CdS materials which are in good agreement with JCPDS cards no. 75-1545. It should be noted that the relative peak intensity of the diffraction arising from (100) plane is much stronger than other

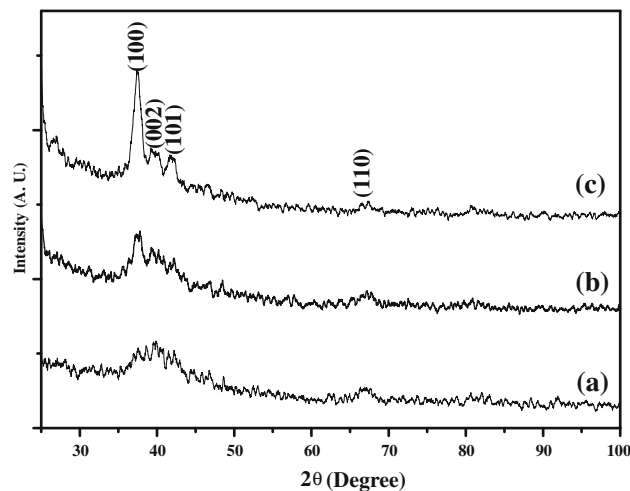


Fig. 2 The XRD patterns of CdS thin films at different thicknesses: (a) 0.13, (b) 0.41, and (c) 1.23 μm

peaks. This shows that CdS films are highly oriented along (100) plane. The grain size along (100) plane was estimated using Scherrer's formula

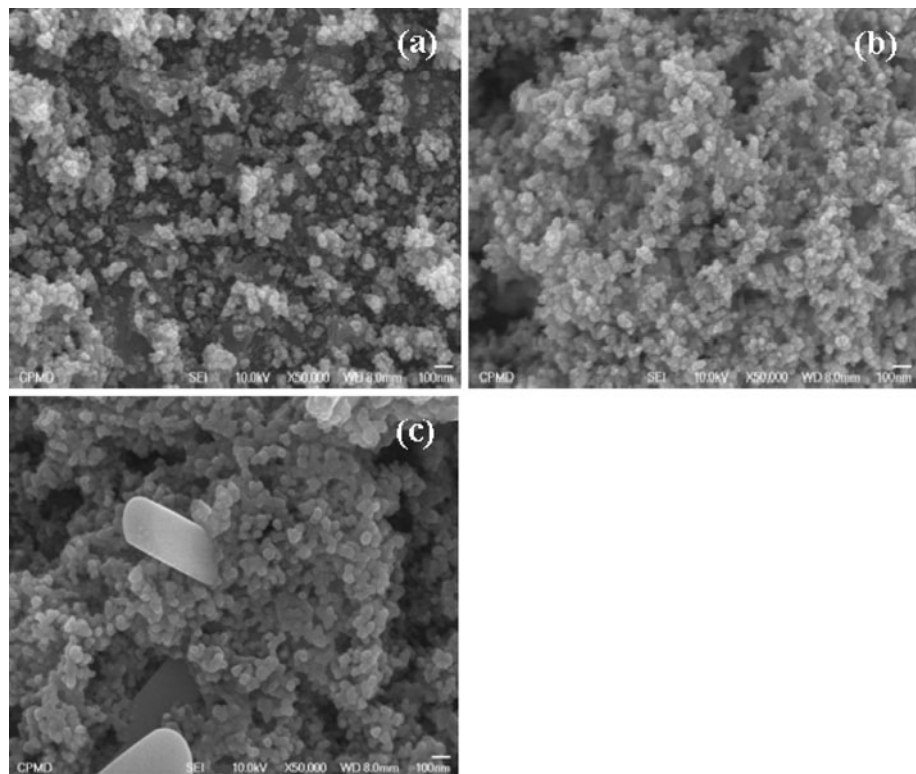
$$D = \frac{0.9\lambda}{\beta \cos\theta} \quad (4)$$

where β is the broadening of diffraction line measured at half maximum intensity (radians) and $\lambda = 2.2897 \text{ \AA}$ is the wavelength of the Cr K α X-ray. The grain size is found to be 14 nm for (100) plane.

Morphological studies

The surface morphologies of the CdS thin films for different thicknesses are shown in Fig. 3a–c at $\times 50,000$ magnification. SEM micrographs reveal the film surfaces are highly porous with some overgrown clusters. This overgrowth can be explained on the basis of nucleation and coalescence process. From the micrographs, one can see that the CdS film of thickness 0.13 μm (Fig. 3a) is composed of the nanocrystalline spherical grains along with some overgrowth of porous spongy clusters. However, the spongy cluster containing nanorods easily seen as the film thickness increases to 0.41 μm (Fig. 3b). Further, increase in thickness (1.23 μm) caused the formation of matured nanorods having diameter 150–200 nm (Fig. 3c), since 160 cycles provides the sufficient time for the growth of grains of relatively larger size. This morphological change is attributed may be due to the presence of excess cadmium in atomic percentage [22]. The barrier effect of intercrystalline CdS is greatly decreased by using long nanorods instead of a porous CdS thin film composed of accumulated nano-sized particles. The morphology of the product was further investigated by TEM analysis. The TEM image having CdS film thickness

Fig. 3 The SEM images ($\times 10,000$) of CdS thin film of different thicknesses: (a) 0.13, (b) 0.41, and (c) 1.23 μm



1.23 μm (Fig. 4a) shows the formation of aggregated as well as interconnected CdS nanorods. Figure 4b is the lattice resolved HRTEM image of the CdS nanorods which indicates that the CdS nanorods are polycrystalline with an individual crystal size of 10–12 nm which is consistent with results obtained from XRD analysis. Figure 4c shows the corresponding selected area electron diffraction (SAED) pattern and it displays the diffused rings confirming the polycrystalline nature. It can be indexed to the reflection of hexagonal crystal structure in crystallography, and this result was also investigated by means of XRD. Electron diffraction reveals that each particle is composed of many small crystal nuclei, which is a convincing proof that the particles grow in an aggregation model.

Surface wettability test

The contact angle is the angle at which a liquid/vapor interface meets the solid surface. The contact angle is specific for any given system and is determined by the interactions across the three interfaces. Most often the concept is illustrated with a small liquid droplet resting on a flat horizontal solid surface. If the liquid is very strongly attracted to the solid surface the droplet will completely spread out on the solid surface and the contact angle will be close to 0° (Hydrophilic). On the other hand, if the solid surface is hydrophobic, the contact angle will be larger than 90° . On highly hydrophobic surfaces, the water

contact angles are as high as 150° or even nearly 180° . On these surfaces, water droplets simply rest on the surface, without actually wetting to any significant extent. In this study, the water lies with contact angle of 105° , 110° , and 130° on the CdS thin film surface for 0.13, 0.41, and 1.23 μm thicknesses, respectively forming a spherical droplet as seen in Fig. 5 indicating hydrophobic behavior. The increase in contact angle with film thickness may be due to increasing porous nature consisting nanorods for CdS thin film as seen from SEM images. Air trapping in the pores of CdS thin films prevents water from adhering to the film results into hydrophobicity of film surface.

Optical studies

The variation of optical absorbance (α) with wavelength (λ) of CdS films for different thicknesses is shown in inset of Fig. 5 and showed that optical absorption decreases with increase in the film thickness. This data was further used for analyzing optical direct band gap energy using following classical relation for near edge optical absorption in semiconductor. The theory of optical absorption gives the relationship between the absorption coefficient “ α ” and the photon energy “ $h\nu$ ” can be written as,

$$\alpha = \frac{A(E_g - h\nu)^n}{h\nu} \quad (5)$$

where “ α_0 ” is a constant, “ E_g ” is the band gap, and “ n ” is equal to 1/2 for a direct and 2 for indirect transition.

Fig. 4 TEM (a), HRTEM (b) and c SAED pattern of CdS nanorod for 1.23 μm film thickness

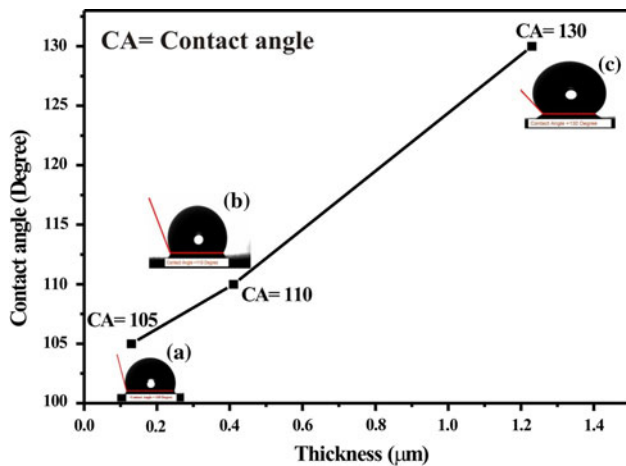
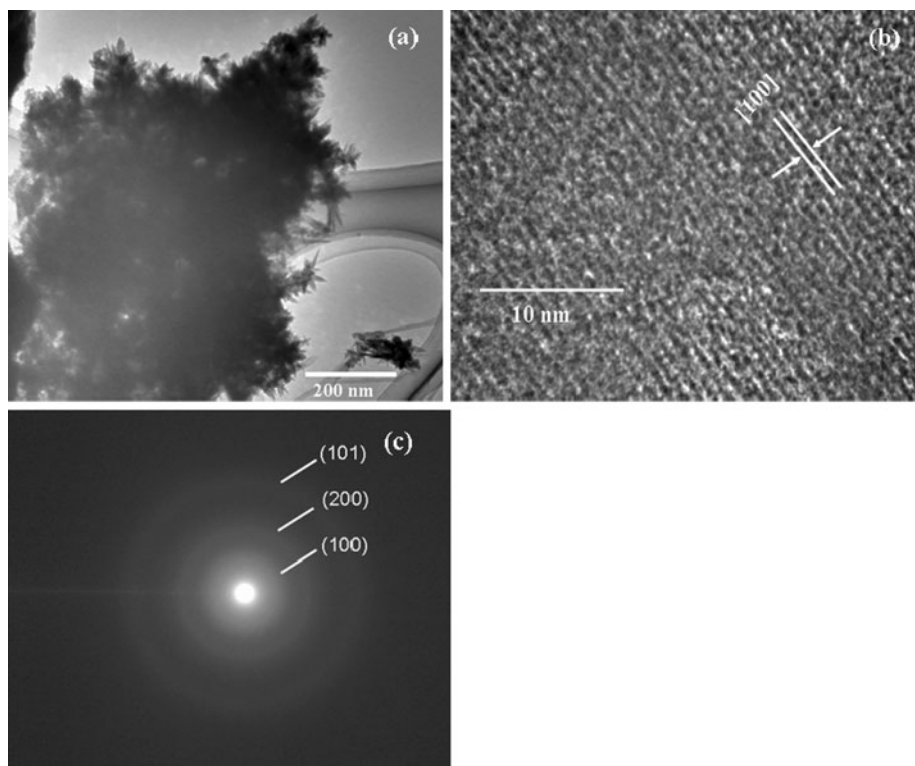


Fig. 5 The variation of contact angle with CdS thin film thickness

Figure 6 shows the plots of $(\alpha h\nu)^2$ versus $h\nu$ for estimating the values of direct band gap energy of CdS films by extrapolating curves to zero absorption coefficient. The band gap energy (E_g) values are found to be 2.02, 2.12, and 2.2 eV for 0.13, 0.41, and 1.23 μm film thickness, respectively, comparable to reported earlier [23, 24]. The increase in direct band gap energy (2.02–2.2 eV) with increase in film thickness is confirmed similar to results reported by Kale et al. [25] and Pathan et al. [26] for CdTe and MnS by using SILAR method, respectively.

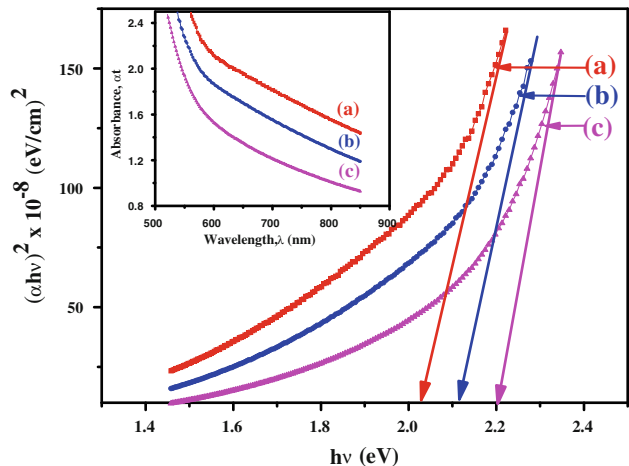


Fig. 6 The variation of $(\alpha h\nu)^2$ with photon energy ($h\nu$) of CdS thin films of different thicknesses: (a) 0.13, (b) 0.41, and (c) 1.23 μm . Inset The variation of absorption (αt) with wavelength (λ) of CdS thin film for the same

Electrical resistivity

The DC electrical resistivity of the CdS thin films was measured as a function of temperature in the range 300–500 K using two-probe method. Figure 7 shows the variation of logarithm of resistivity with reciprocal of temperature for the CdS thin films with different thicknesses. The electrical resistivity is decreased with increase in temperature, indicating the semiconducting behavior of

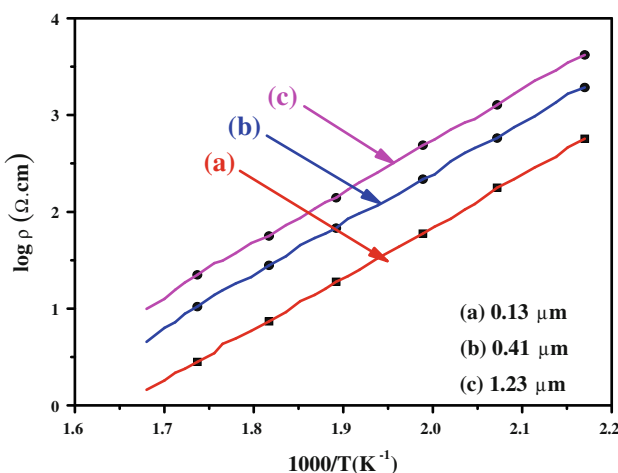


Fig. 7 The variation of $\log \rho$ with $(1000/T)$ for CdS thin films of different thicknesses: (a) 0.13, (b) 0.41, and (c) 1.23 μm

CdS thin films. A room temperature (300 K) electrical resistivity of CdS films are found to be in the range of 10^4 – $10^6 \Omega \text{ cm}$ for different thicknesses. These values are in good agreement with earlier reported [18, 27].

Thermo-emf measurement

The plot of thermo-emf with temperature for the CdS thin films with different thickness is shown in Fig. 8. In the thermo-emf measurement, the temperature difference causes the transport of carriers from the hot end to the cold end and thus creates an electric field, which gives the thermal voltage. This thermally generated voltage is directly proportional to the temperature difference created across the semiconductor. In this case, thermo-emf was measured as a function of temperature in the range 300–500 K, using two-probe method. The polarity of the induced emf for CdS

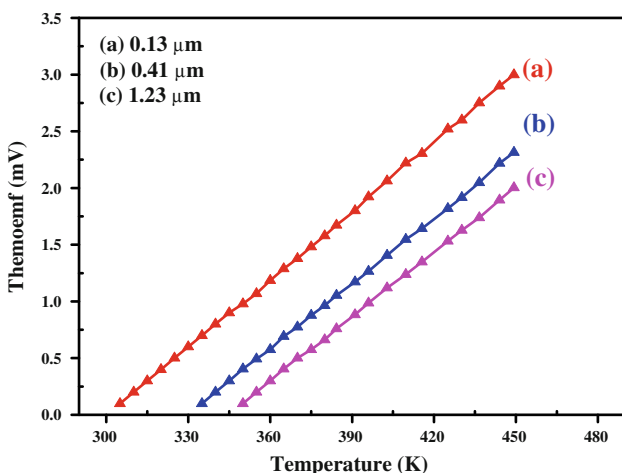


Fig. 8 The variation of thermo-emf with temperature of CdS thin films of different thicknesses: (a) 0.13, (b) 0.41, and (c) 1.23 μm

film indicated n-type electrical conductivity, similar to earlier reports for CdS thin films [28].

Conclusions

Polycrystalline CdS nanorods have been prepared onto glass substrates by simple and inexpensive SILAR method. The XRD studies showed that the CdS possesses hexagonal crystal structure with high orientation along (100) plane. The surface morphological study revealed that the CdS thin film surface is composed of the nanocrystalline spherical grains along with some overgrowth of porous spongy clusters and increase in thickness causes the formation of matured nanorods having diameter 150–200 nm. The optical studies showed that the band gap energy values are 2.02, 2.12, and 2.2 eV for 0.13, 0.41, and 1.23 μm film thicknesses, respectively. The CdS films showed the semiconducting behavior with room temperature electrical resistivity in the range of 10^4 – $10^6 \Omega \text{ cm}$ and have n-type electrical conductivity.

Acknowledgements The authors are grateful to the Department of Science and Technology, New Delhi for financial support through the scheme no. SR/S2/CMP-82/2006.

References

- Bose S, Saha SK (2003) Chem Mater 15:4464
- Cushing B, Kolesnichenko VL, O'Connor CJ (2004) Chem Rev 104:3893
- Trindade T, O'Brien P, Pickett NL (2001) Chem Mater 13:3843
- Dushkin CD, Saita S, Yoshie K, Yamaguchi Y (2000) Adv Colloid Interface Sci 88:37
- Banerjee R, Jayakrishnan R, Ayyub P (2000) J Phys Condens Matter 12:10647
- Alivisatos AP (1996) Science 271:933
- Hall RB, Meakin JB (1979) Thin Solid Films 63:203
- Dimmler B, Schock HW (1996) Prog Photovolt 4:425
- Britt J, Ferekides C (1993) Appl Phys Lett 62:2851
- Arai T, Yoshida T, Ogawa T (1987) J Appl Phys 26:396
- Lianos P, Thomas JK (1986) Chem Phys Lett 125:299
- Bosale BM, Tseng EJ, Lo DS (1985) US Patent 4:548
- Kale SS, Jadhav US, Lokhande CD (1996) Ind J Pure Appl Phys 34:324
- Dhawale DS, Dubal DP, Deokate RJ, Gujar TP, Sun YK, Lokhande CD (2010) J Alloys Comp 503:422
- Chamberlain RR, Skarmann J (1996) J Electrochem Soc 113:86
- Matsumoto H, Nakayamm A, Ikegami S, Hiroi Y (1980) Jpn J Appl Phys 15:129
- Nicolau YF, Dupuy M (1990) J Electrochem Soc 137:2915
- Sankapal BR, Mane RS, Lokhande CD (2000) Mater Res Bull 35:177
- Lokhande CD, Sankapal BR, Pathan HM, Muller M, Gersig M, Tributsch H (2001) Appl Surf Sci 7188:1
- Salunkhe RR, Dhawale DS, Gujar TP, Lokhande CD (2009) Mater Res Bull 44:364
- Sasikala G, Dhanasekaran R, Subramanian C (1997) Thin Solid Films 302:71

22. Ristic M, Popovic S, Music S (2004) Mater Lett 58:2494
23. Patidar D, Sharma R, Jain N, Sharma TP, Saxena NS (2006) Bull Mater Sci 29:21
24. Kumar V, Sharma SK, Sharma TP, Singh V (1999) Opt Mater 12:119
25. Kale SS, Mane RS, Pathan HM, Shaikh AV, Joo OS, Han SH (2007) Appl Surf Sci 253:4335
26. Pathan HM, Kale SS, Lokhande CD, Han SH, Joo OS (2007) Mater Res Bull 42:1565
27. Lokhande CD (1990) Mater Chem Phys 34:324
28. Pathan HM, Lokhande CD (2004) Bull Mater Sci 27:85